Development of high-efficiency and low-cost unshrouded turbine runner for small scale hydropower plant

IOP Conf. Series: Earth and Environmental Science **240** (2019) 022055 doi:10.1088/1755-1315/240/2/022055

Development of high-efficiency and low-cost unshrouded turbine runner for small scale hydropower plant

T Aida[1], Y Nakamura[2], and K Miyagawa[3]

1 Engineering Division, Tanaka Hydropower Co., Ltd., Kanagawa, 2430215, Japan
2 Department of Applied Mechanics, Waseda University, Tokyo, 1690072, Japan
3 Department of Applied Mechanics and Aerospace Engineering, Research Institute for Science and Engineering, Waseda University, Tokyo, 1690072, Japan

Email: takamitsu-aida@tanasui.co.jp

Abstract. Facing a growing demand for low initial cost and high-efficiency small scale hydropower plants, a new type of Francis turbine was developed for Kazunogawa small hydropower plant with cooperation from industrial, governmental, and academic sectors. To reduce the cost of the turbine while increasing its efficiency, a prototype turbine with an unshrouded runner and a cylindrical casing was developed. The unshrouded runner was designed by Waseda University. Typically, the turbine runner for small scale hydropower is manufactured via a casting method; however, the unshrouded runner can be milled with a 5 axis CNC machine, thereby reducing cost and manufacturing lead time. A cylindrical casing has advantages of low fabrication cost and compact footprint. However, it had lower efficiency compared to a spiral casing with conventional design. Therefore, in this study, topology optimization based on CFD analysis was conducted on the casing and double circular cascade to improve efficiency. In addition, the axial thrust was estimated from CFD analysis to design the bearings and to determine the runner gap. Finally, a performance test was conducted on-site and peak efficiency of 91% was confirmed. This paper also reports the follow-up observation of the prototype turbine after commercial operation started.

1. Introduction

Among the renewable energies, small hydroelectric power generation has garnered much attention since there are still thousands of potential sites that can be developed with minimum environmental impact. The key to the development of these potential sites is its economic feasibility, which can be directly tied to the initial plant cost and turbine efficiency.

Nakamura et al. proposed an unshrouded Francis runner which meets the requirement for low cost manufacturing and high turbine efficiency [1, 2]. Its peak efficiency of 88% was validated via model turbine testing at Waseda University. For this model turbine, a typical spiral casing was adopted.

The purpose of this study is to develop a low-cost and high-efficiency prototype turbine adopting an unshrouded runner and a cylindrical casing. A cylindrical casing has no miter bends. Therefore, many manufacturers can fabricate it at a lower cost. Also, since it has a compact footprint, the construction cost can be reduced. However, a cylindrical casing with the conventional design had a lower efficiency. Stay vanes, guide vanes and a draft tube were newly designed to adopt a cylindrical casing. Only the runner was simply scaled to the size of the prototype turbine. To characterize the loss mechanism and to improve the efficiency of the cylindrical casing and double circular cascade, CFD analysis was performed.

2. Hydro turbine specification

The specifications of the model turbine and prototype turbine which was installed at Kazunogawa small hydropower plant are listed in Table 1. Figure 1 shows the unshrouded runner which was fabricated by a 5 axis CNC machine. Figure 2 shows a cut section of the model turbine. Figure 3 shows the fully assembled prototype turbine.

Table 1. Hydro turbine specifications.

	Model	Prototype
Flow rate	0.056 m^3/s	0.25 m^3/s
Effective head	16m	86m
Rotational speed	900 rpm	1500 rpm
Rated power	7.9kW	160kW
Specific speed	79.2 m-kW	79.2 m-kW
Runner outlet diameter	0.164 m	0.224 mm
Reynolds number	1.3 x 10^6	3.9 x 10^6

Figure 1. Unshrouded runner.

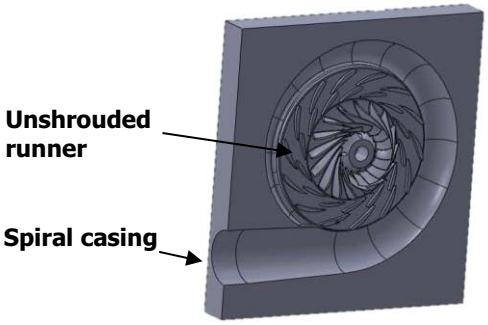

Figure 2. Cut section of model turbine.

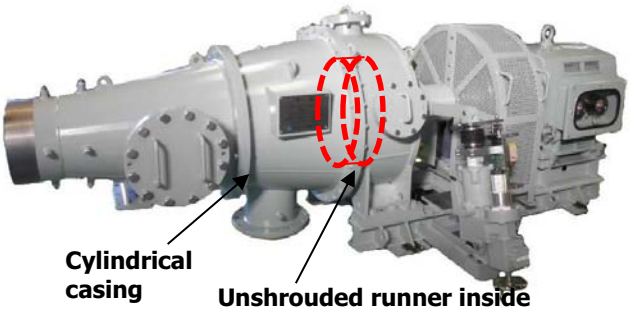

Figure 3. Overview of prototype turbine.

3. Topology optimization for casing and double circular cascade based on CFD

To analyze the internal flow and loss mechanism inside the casing, steady state integral flow computation was performed using a general-purpose code ANSYS-CFX15.0, Reynolds-Averaged Navier-Stokes equation and SST k-ω turbulence model. The mesh number was about two million. The boundary conditions were the total pressure at the inlet and the static pressure at the outlet. Figure 4 shows the domains and mesh of the analysis model. The shape modifications were carried out by the following 2 steps. For step1, the flow from the casing inlet to the stay vanes inlet was modified. For step 2, the flow at the double circular cascade, composed of stay vanes and guide vanes, was modified.

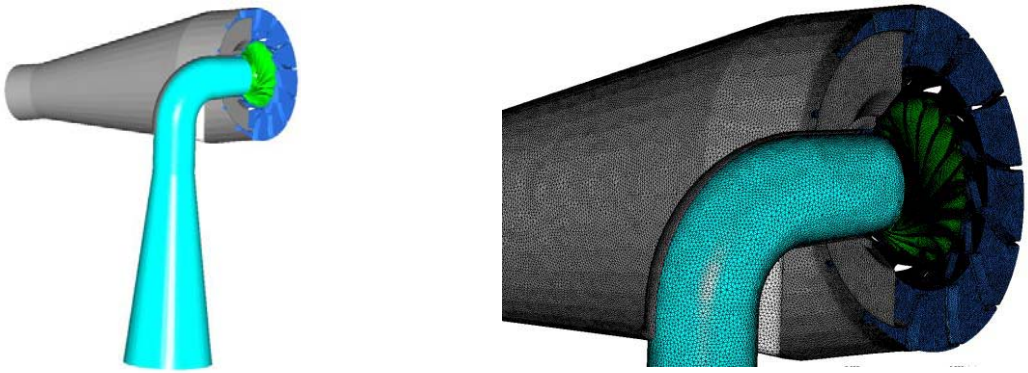

Figure 4. Mesh and domains for CFD analysis.

3.1. Step 1: The flow from casing inlet to stay vane inlet.

The effect of the casing inlet angle was analysed by comparing a 20 degree angle versus a 10 degree angle. Conventional cylindrical casings typically have a large spread angle of 20 degrees at the inlet. Figure 5(a) shows total pressure distribution and velocity vectors of the conventional casing. From the result, it is apparent that the flow separates at the inlet and causes total pressure loss. As shown in Figure 5(b), at a spread angle of 10 degrees, flow separation was mitigated.

Also, flow path width at the stay vane inlet was modified. Figure 6(a) shows a conventional design and there is flow separation seen at the edge of the casing disk. For the prototype turbine, the diameter of the casing disk was decreased by 100mm to secure enough path width so that the flow velocity decreases and mitigates flow separation as shown in Figure 6(b).

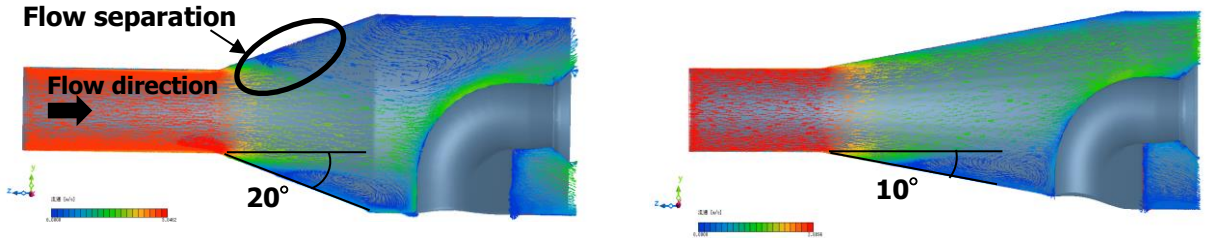

(a) Conventional casing (20 degree). (b) Modified casing (10 degree).

Figure 5. Total pressure and vectors at casing inlet.

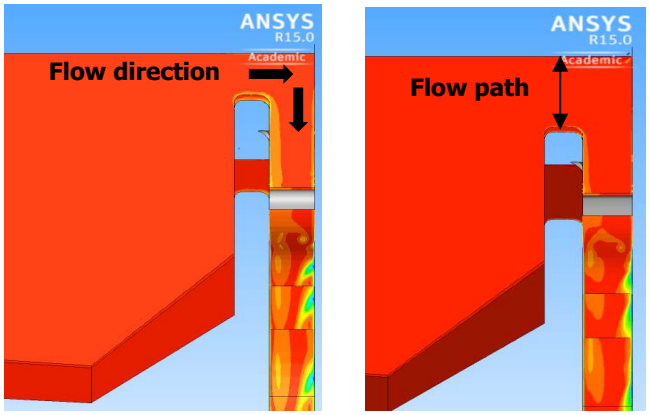

(a) Conventional casing. (b) Modified casing.

Figure 6. Total pressure at stay vane inlet.

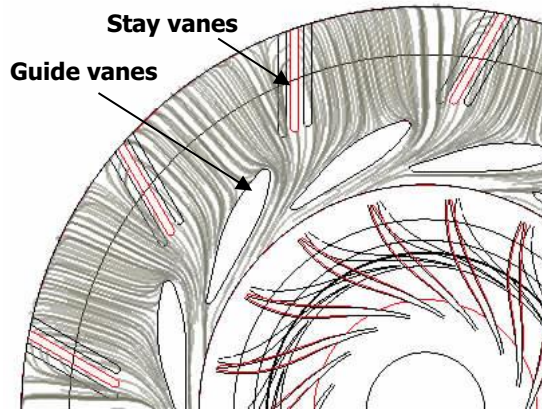

Figure 7. Streamline in double circular cascade.

3.2. Step 2: The flow at the double circular cascade

Unlike a spiral casing, a cylindrical casing does not give any angular momentum to the flow. Figure 7 shows the streamline at the double circular cascade with a conventional casing. In the conventional casing, these stay vanes are straight for easier fabrication. As the shown in this figure, the stay vanes allow the flow near the midpoint of the stay vane pitches to exhibit minimal flow rectification when inflowing into the guide vanes.

To improve efficiency, the following parameters were compared; (1) relative position of the stay vanes and guide vanes, (2) length of the stay vanes and (3) inlet and outlet angles of the stay vanes. CFD analysis was carried out with these parameter patterns as shown in Table 2.

Figure 8 shows the results of total pressure loss in each case. The effect of the relative circumferential position of the stay vanes and guide vanes were compared amongst case 1, 2 and 3. From the results, case 3 shows the smallest total pressure loss. The effect of the stay vane length was compared between case 2 and 4. Figure 9 shows the total pressure distribution of each case. Case 4 shows lower loss because the wake flow at the stay vanes is smoother and it decreases the guide vane

loss. The effect of the angles of the stay vanes were compared between case 4 and 5. Figure 10 shows the total pressure distributions of each case. In Figure 10(b), a vortex occurs at the back side of the stay vanes and it causes total pressure loss. It is assumed that the inlet angle should be 90 degrees for the cylindrical casing to mitigate the pressure loss.

Table 2. Parameter patterns for CFD analysis.

Case	1	2	3	4	5
Relative position (deg)	-5	0	5	0	0
SV length	short	short	short	long	long
SV angle (deg)	90 to 60	90 to 60	90 to 60	90 to 60	60 to 25

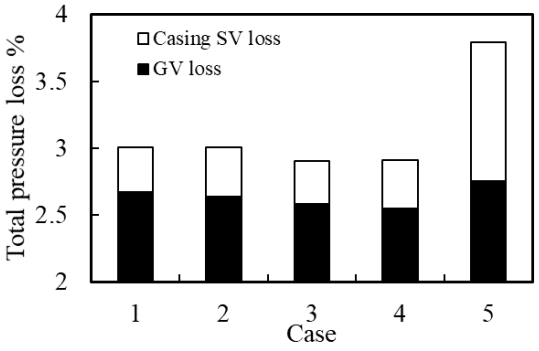

Figure 8. Total pressure loss on each case.

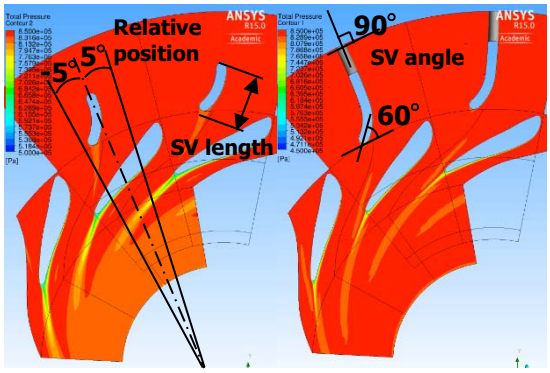

(a) Case 2. (b) Case 4.

Figure 9. Total pressure at mid plane.

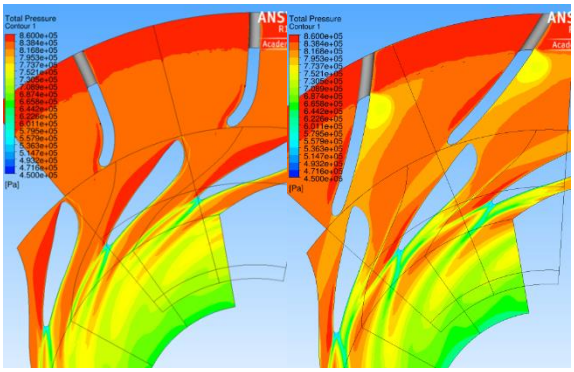

(a) Case 4. (b) Case 5.

Figure 10. Total pressure at shroud side.

Based on the results above, it can be inferred that case 3 with the long stay vanes is the best parameter setting. With these parameters, three different types of guide vanes were compared. Each type has a different inlet angle but the same outlet angle. The parameters are listed on Table 3. Figure 11 shows the results of total pressure loss and Figure 12 shows the total pressure distribution. On Figure 12(a) and (c), the inlet flow to the guide vanes turns to their rear side which causes total pressure loss. Based on the results, case 2 was adopted for the prototype turbine.

Table 3. Guide vane parameters.

Case	1	2	3
Shape	Conventional	Reverse	Symmetrical
Inlet angle	30 deg	56.5 deg	35 deg
Outlet angle	17 deg	17 deg	17 deg

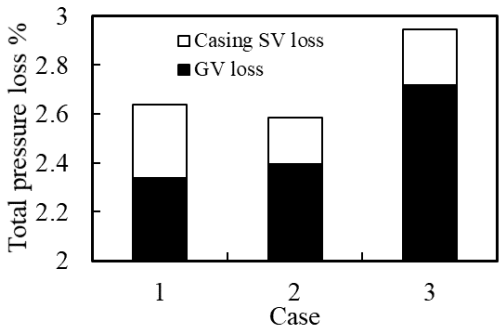

Figure 11. Total pressure loss.

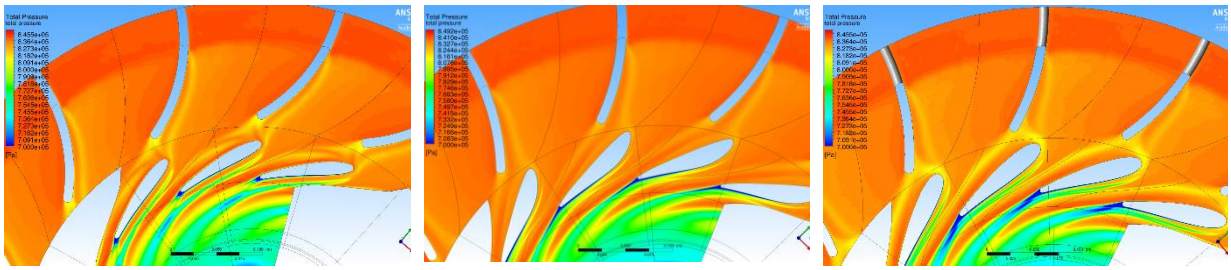

(a) Case 1. (b) Case 2. (c) Case 3.

Figure 12. Total pressure distribution at double circular cascade.

4. Axial thrust estimation based on CFD

It is important to estimate the axial thrust to design turbine bearing specifications and to determine the proper runner gap while maximizing volumetric efficiency. CFD analysis on runner back side was conducted to calculate axial thrust. Figure 13 shows the pressure distribution and by integrating pressure on the surface, the axial thrust was calculated as 58.8kN towards the draft side. Also, the axial direction force of the runner surface was -27.5kN. Therefore, the estimated axial thrust is 31.3kN towards the draft side direction. Considering the axial gap of the bearings, it was confirmed that the axial displacement will not exceed 0.3mm. The runner gaps were determined as shown in Figure 14. The minimum axial gap is 0.3mm at the partial band which protects the runner blades from contact.

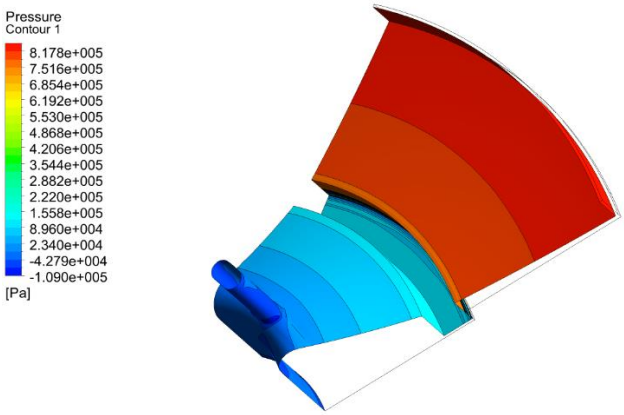

Figure 13. Pressure distribution on runner rear side.

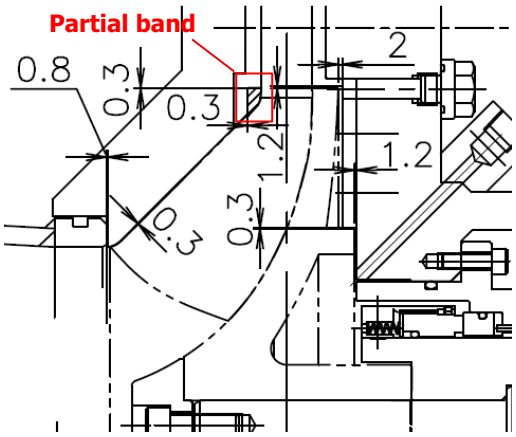

Figure 14. Designed runner gap.

5. Performance test on prototype turbine

Load rejection test and efficiency test on the prototype turbine were performed at Kazunogawa small hydropower plant in Yamanashi prefecture. Figure 15 shows the measurement points. The pressure and the rotational speed were measured by pressure transmitter and a non-contact tachometer. Also, the flow rate was measured by an ultrasonic flowmeter placed at the penstock.

The load rejection tests were performed four times at each generator output of 40, 80, 120 and 146kW. Figure 16 shows the results of the load rejection test at the maximum output of 146kW. In this figure, all measured values are normalized with steady state values. Figure 16 shows the runaway speed on each output compared with the predicted value from the model test. As the result, the runaway speed was below the predicted line within the entire region. The measured values diverge from the predicted line at small GV openings because the prototype turbine has a flywheel and the moment of inertia is much larger than the model turbine. Therefore, the guide vanes shut before it reached maximum runaway speed at each GV opening.

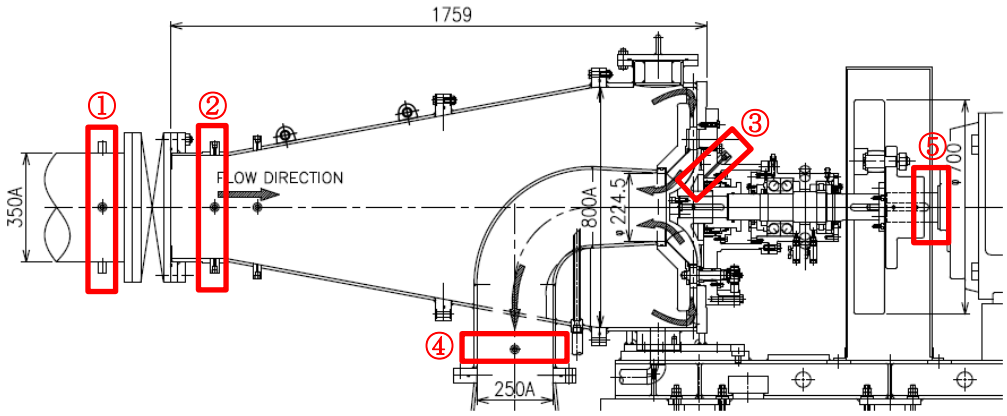

④ Penstock pressure. ② Casing pressure. ③ Runner back pressure.
④ Draft pressure. ⑤ Rotational speed.

Figure 15. Overview of measurement points.

Figure 18 shows the results of efficiency test in comparison to the CFD analysis results. The peak turbine efficiency of 91% was verified on the prototype turbine. It is about 3% higher than the model test result. Also, the peak efficiency was observed at the designed point.

The runner back pressure was measured during continuous operation at 100% GV opening. Figure 19 shows the measured value in comparison with the pressure distribution from the CFD result. The pressure is normalized by steady state pressure at the casing inlet. This result indicates that the axial thrust estimation was accurate.

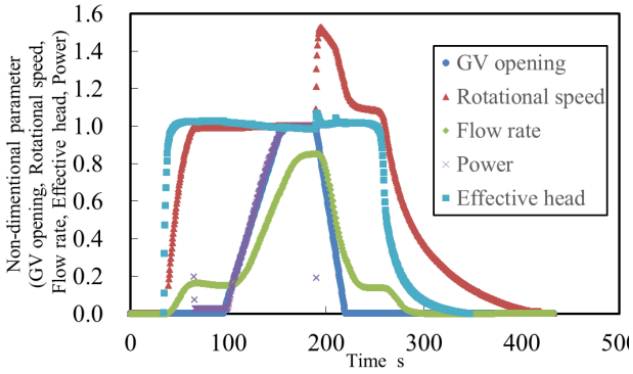

Figure 16. Results of load rejection test.

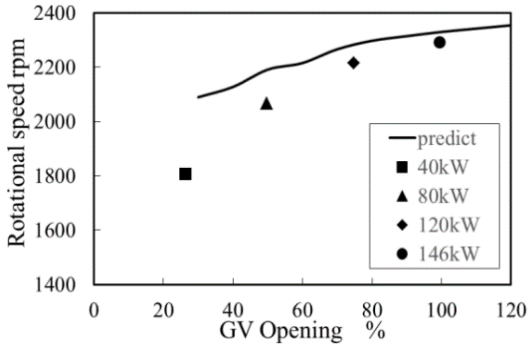

Figure 17. Comparison of runaway speed.

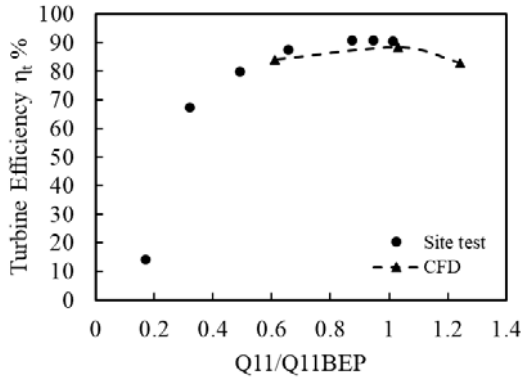

Figure 18. Result of efficiency test.

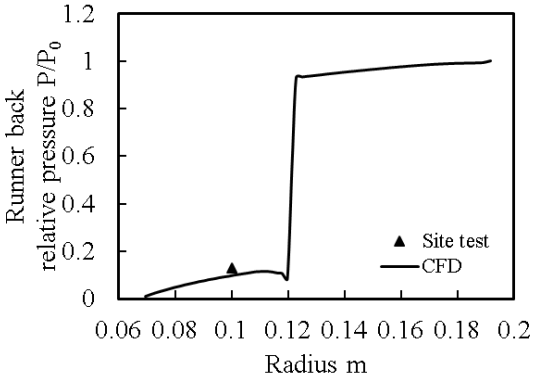

Figure 19. Comparison of runner back pressure.

6. Follow-up observation after commercial operation

The commercial operation of the prototype turbine started on December 19, 2014. After 250 days of operation, the first internal inspection was conducted. The second internal inspection was conducted 930 days after the first inspection.

According to the model test, cavitation at the runner blade tips was a matter of some concern. From the experimental and CFD results, unique cavitation phenomena were observed at the runner blade tips as shown in Figure 20. Two runners of different materials, AlBC and SUS304, were fabricated to compare the cavitation intensity. The AlBC runner was operated 250 days and the SUS304 runner was operated 930 days and there was no sign of cavitation erosion on either runner surface.

Given the initial concerns of cavitation at the runner blade tips, it was determined that the casing surface needed to be protected. The casing is made of SS400. To improve cavitation intensity, tungsten carbide(WC-10Ni) powders were sprayed by an HVOF thermal spraying apparatus to the opposing casing surface of the runner blade tips. HVOF thermal spraying provides denser and smoother coating with minimum porosity. Also, tungsten carbide is widely used to improve cavitation corrosion resistance.

However, during the first inspection, peeling of the coating was observed as shown in Figure 21. Corrosion was observed at the entire boundary surface and the remaining coating was easily peeled off by tapping it with a hammer. It is assumed that water seeped into the pores due to insufficient sealing treatment causing galvanic corrosion between the SS400 and tungsten carbide.

As a result, the coating material of the thermal spray was changed to Ni-20Al to prevent galvanic corrosion. After the Ni-20Al coating was applied, there was no peeling observed after 930 days operation.

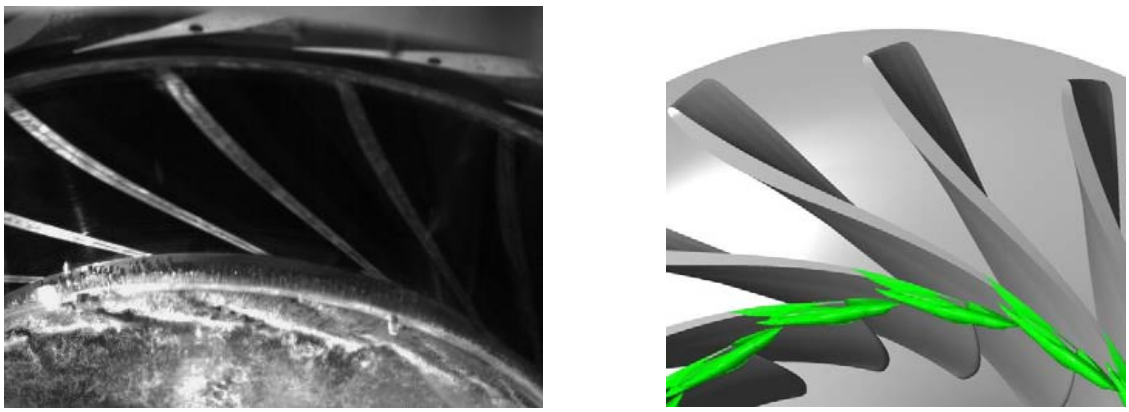

(a) Experimental result. (b) CFD result (void fraction=0.1).

Figure 20. Cavitation appearance (N_{11}/N_{11BEP}=1.0, Q_{11}/Q_{11BEP}=1.0, σ =0.05).

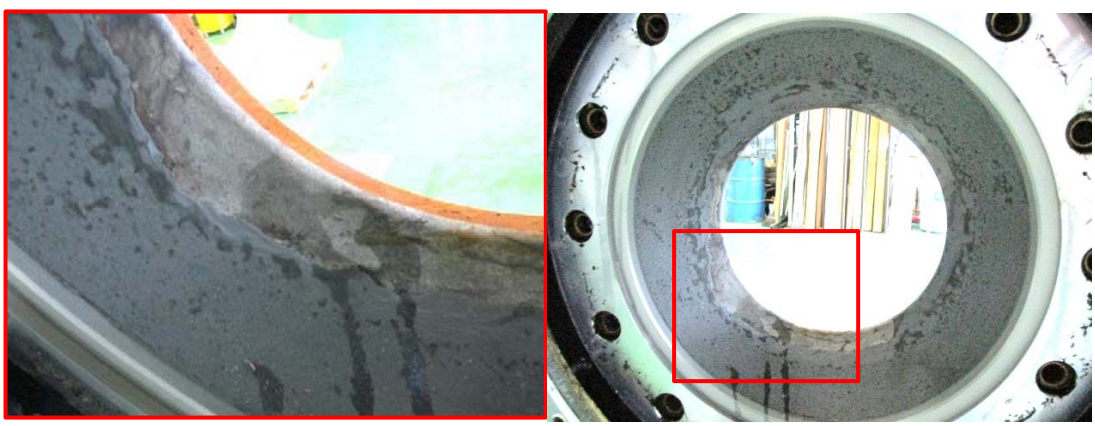

Figure 21. Peeling of the tungsten carbide coating.

7. Conclusion

A low-cost and high-efficiency turbine with an unshrouded runner and a cylindrical casing was developed and tested. The prototype turbine started commercial operation on December 2014 and is still operating without major issues.

- An unshrouded runner was adopted to reduce manufacturing cost
- A cylindrical casing was adopted to reduce manufacturing and construction costs.
- The internal flow of a cylindrical casing including double circular cascade was clarified and modified accordingly.
- In the load rejection test, the runaway speed did not exceed predicted speed.
- In the efficiency test, the peak turbine efficiency of 91% was observed at the designed point.
- Two runners were fabricated. One using AlBC and the other SUS304. There was no sign of cavitation erosion on either runner.
- Two materials were used for thermal spray coating. A tungsten carbide coating resulted in peeling possibly due to galvanic corrosion. There was no peeling observed when utilizing a nickel aluminide coating.

Acknowledgement

This study was supported by New Energy Foundation and carried out in collaboration with various company and university. The authors would like to express their sincere gratitude to Tokyo Electric Power Co., Inc; Kandenko Co., Ltd and Heiwa Sangyo Co., Ltd.

References

[1] Nakamura Y, Shima R, Komatsu H, Shiratori S and Miyagawa K (2015, July). Development of Shroudless Francis Turbine. In *ASME/JSME/KSME 2015 Joint Fluids Engineering Conference* (pp. V01AT02A006-V01AT02A006). American Society of Mechanical Engineers.

[2] Nakamura Y, Komatsu H, Shiratori S, Shima R, Saito S and Miyagawa K (2015, November). ICOPE-15-1164 Development of high-efficiency and low-cost shroudless turbine for small hydropower generation plant. In *The Proceedings of the International Conference on Power Engineering (ICOPE) 2015.12* (pp. _ICOPE-15). The Japan Society of Mechanical Engineers.